



Spectroscopic and electrochemical properties of heteroleptic cationic copper complexes bis-(diphenylphosphino)alkane-(2,2'-biquinoline)copper(I). Crystal structure of bis(diphenylphosphino)ethane-(2,2'-biquinoline)copper(I) perchlorate

Juan Guerrero^{a,*}, Luis Cortez^a, Luis Lemus^a, Liliana Farías^a, Juan Costamagna^a, Claudio Pettinari^b, Miriam Rossi^c, Francesco Caruso^d

^a Faculty of Chemistry and Biology, Universidad de Santiago de Chile, Santiago 33, Chile

^b Dipartimento di Scienze Chimiche, Università di Camerino, via S. Agostino 1, 62032 Camerino, MC, Italy

^c Vassar College, Department of Chemistry, Poughkeepsie, NY 12604-0484, USA

^d Istituto di Chimica Biomolecolare (ICB-CNR), Università di Roma "La Sapienza", Istituto Chimico, Ple Aldo Moro 5, 00185 Rome, Italy

ARTICLE INFO

Article history:

Received 25 April 2010

Received in revised form 30 June 2010

Accepted 12 July 2010

Available online 21 July 2010

Keywords:

Heteroleptic copper (I) complexes
Biquinoline and bis-diphenylphosphinoalkane ligands
Spectroscopic properties
X-ray crystal structure

ABSTRACT

A series of $[\text{Cu}^{\text{I}}(2,2'\text{-biquinoline})(\text{L})](\text{ClO}_4)$ complexes ($\text{L} = \text{bis}(\text{diphenylphosphino})\text{methane}$ (**bppm**), 1,2-bis(diphenylphosphino)ethane (**bppe**), 1,4-bis(diphenylphosphino)butane (**bppb**)) have been synthesized and characterized by elemental analysis, conductivity, ESI-mass, NMR and UV–Vis spectroscopies, cyclic voltammetry, X-ray diffraction ($[\text{Cu}^{\text{I}}(2,2'\text{-biquinoline})(\text{bppe})](\text{ClO}_4)$) and DFT calculations. These compounds are monometallic species in a distorted tetrahedral arrangement, in contrast with related compounds found as dinuclear according to diffraction studies. The spectroscopic properties are not directly correlated with the length of alkyl chain bridge between the bis-diphenylphosphine groups. In this way, the chemical shift of some 2,2'-biquinoline protons and the metal to ligand charge transfer (Cu to 2,2'-biquinoline) follows the order $[\text{Cu}(2,2'\text{-biquinoline})(\text{bppm})](\text{ClO}_4)$, $[\text{Cu}(2,2'\text{-biquinoline})(\text{bppb})](\text{ClO}_4)$, $[\text{Cu}(2,2'\text{-biquinoline})(\text{bppe})](\text{ClO}_4)$. The same dependence is followed by the potentials to Cu(II)/Cu(I) couple. These results are discussed in terms of inter-phosphorus alkane chain length and tetrahedral distortions on copper.

© 2010 Elsevier B.V. All rights reserved.

1. Introduction

The interest in studying the behavior of coordination compounds of copper(I) with polypyridine ligands arises from their application either in catalysis [1], bioinorganic systems [2], and photochemical research [3] among other areas [4]. Several studies have shown that in four-coordinated copper(I) complexes, either their electronic properties as well as their reactivity (as a consequence of the former), are affected by dynamic behavior related to the conformational flexibility of these complexes in solution. In this way, distortions of the ideal tetrahedral coordination geometry toward an extreme square-planar geometry, drive to a diversity of processes, such as: modification of redox properties, decoordination of ligands and in some cases *equilibria* between different copper(I) species [5].

The effect of coordination geometry over properties of copper(I) complexes can be understood through the modification of the molecular orbitals as the ligands induce distortions of the ideal tetrahedral structure required by the copper(I) ion. For example,

in homoleptic copper(I) complexes with phenanthroline ligands, the geometry varies from D_{2d} to D_2 by loss of symmetry, modifying the energy of the HOMO, as shown through the shift of metal to ligand charge transfer band in their electronic spectra [3e,6].

The geometry of copper(I) complexes may also be modulated by ligands allowing a less restricted way of coordination around the metal center and potential distortion of the tetrahedral arrangement [3,7].

Considering a conformation distant from the ideal tetrahedron, it is expected that a more distorted geometry would reduce the necessary energy to reach a square-planar geometry, which is optimum for Cu(II) complexes, modifying favorably the oxidation potentials when the variable factor is the flattening conformation in a series of copper(I) complexes [7,8]. For example, photo-physical studies show that the flattening distortion in polypyridine copper(I) complexes reduces their emissive properties, which can be improved by the use of more rigid ligands or with substituents that avoid distortions from the tetrahedral geometry [6].

On the other hand, heteroleptic copper(I) complexes show interesting photo-physical properties, when chelating diphosphines are used together to polypyridine ligands [3c,9]. Also, tertiary phosphines have been selected as ligands to play a major

* Corresponding author. Tel.: +56 2 7181057.

E-mail address: juan.guerrero@usach.cl (J. Guerrero).

role in the stabilization of low oxidation states in transition metals [5b].

To evaluate the role of ligand flexibility in the conformation of copper(I) complexes, we have studied three heteroleptic complexes, where the ligands are the high electron-delocalized 2,2'-biquinoline (**biq**), and a series of three chelating alkyl diphosphines with inter-phosphorus bridge of variable length: bis-(diphenylphosphine)methane (**bppm**); 1,2-bis(diphenylphosphine)ethane (**bppe**); 1,4-bis(diphenylphosphine)butane (**bppb**), see Fig. 1.

The effect of structural factors such as distortions of the tetrahedral environment of copper(I) and the length of the inter-phosphorus alkane chain, among others are presented and discussed to explain the changes observed in NMR, UV-Vis spectra and cyclic voltammograms for this series of copper(I) complexes.

2. Experimental

2.1. Instrumental

Analysis of C, H and N were performed using a Fisons element analyzer, model EA-1108. Molar conductivities were obtained from 10^{-3} mol/L solutions in acetone at 25 °C using a Cole-Palmer conductivity meter, model 01481. The positive and negative electro spray mass spectra were obtained with a Series 1100 MSI detector HP spectrometer, using an acetonitrile mobile phase. Solutions (3 mg/mL) for electro spray ionization mass spectrometry (ESI-MS) were prepared using reagent-grade acetonitrile.

Electronic spectra were measured on an Analytik Jena Specord S-100 spectrophotometer at room temperature, from 1.5×10^{-5} mol/L solutions in acetone, tetrahydrofuran and chloroform.

^1H , $^{31}\text{P}\{^1\text{H}\}$ NMR, ^1H - ^1H 2D-COSY and ^1H - ^1H 2D-NOESY spectra were recorded on a Bruker Avance 400 MHz spectrometer (400.133 MHz for ^1H , 160.984 MHz for ^{31}P) equipped with a 5 mm multinuclear broad-band dual probehead, incorporating a z-gradient coil. All the measurement were done in CDCl_3 at 300 K. Chemical shifts (in ppm) for ^1H , were calibrated respect to the residual protonated signal of the solvent (CHCl_3 , 7.26 ppm) and reported relative to Me_4Si . $^{31}\text{P}\{^1\text{H}\}$ spectra were calibrated respect to the external pattern H_3PO_4 10%.

Cyclic voltammetry measurements were carried out using a Voltalab PGZ-100 equipment, supplied with the analyzer software Voltmaster-4. The electrolytic cell used was a conventional three-

compartment cell, provided with a glass carbon working electrode, a Pt auxiliary electrode and a AgCl/Ag reference electrode. The CV measurements were performed at room temperature and N_2 atmosphere, using solutions 1×10^{-3} mol/L of the complexes and 0.10 mol/L of tetraethylammonium perchlorate as supporting electrolyte in CH_3CN as solvent, and scan rates of 20 and 100 mV s^{-1} . The potentials were informed as $E_{1/2}$ versus Ag/AgCl.

Red crystals of $[\text{Cu}^{\text{I}}(\text{biq})(\text{bppe})](\text{ClO}_4)$ were grown by slow diethyl ether diffusion into a solution of the complex in dichloromethane, under N_2 atmosphere. A Bruker Apex-2 diffractometer was used with Mo $\text{K}\alpha$ graphite-monochromatized radiation to collect data on a suitable crystal at 125 K. Diffracted beams were measured using a CCD detector. Crystal and data collection details are given in Table 1. The structure was solved by the heavy-atom method using CAOS [10] and refined by full-matrix least-squares procedures on F . Hydrogen atoms were located by model according to C-H = 0.96 Å and refined riding on their attached atoms.

The theoretical study involved calculations using software programs from ACCELRYS [11]. Density functional theory (DFT) code DMol3 was applied to calculate energies and optimize geometries; graphical displays were generated with Materials Studio Visualizer [12]. We employed Double Numerical Polarized (DNP) basis set that includes all the occupied atomic orbitals plus a second set of valence atomic orbitals plus polarized d-valence orbitals [11]. Correlation generalized gradient approximation (GGA) was applied in the manner suggested by Perdew-Burke-Ernzerhof (PBE) [13]. Spin unrestricted approach was exploited with all electrons being considered explicitly. The real space cutoff of 4 Å was imposed for numerical integration of the Hamiltonian matrix elements. The self-consistent-field convergence criterion was set to the root-mean square change in the electronic density to be less than $10^{-6} \text{ e } \text{Å}^{-3}$. The convergence criteria applied during geometry optimization were $2.72 \times 10^{-4} \text{ eV}$ for energy and $0.054 \text{ eV } \text{Å}^{-1}$ for force. Calculations were performed using X-ray coordinates of the **bppe** compound as starting data. The minimum obtained was later modified to establish a methylene or a tetramethylene bridge for the **dppm** and **dppb** complexes, respectively. In the latter case, the bridge was widely varied to avoid being trapped in minima of higher energy. The minimum nature of these converged structures was checked by calculating the corresponding frequencies and so data shown in Table 3 do not have any associated imaginary frequency.

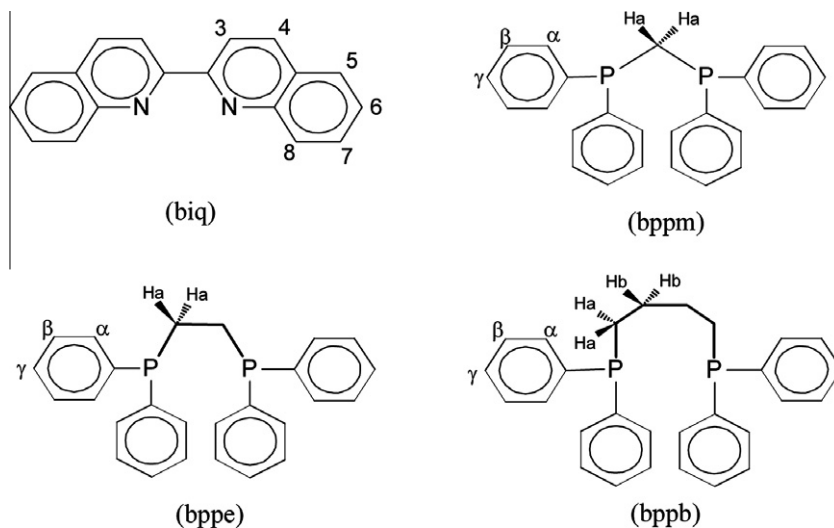


Fig. 1. Structure and numbering for protons of the ligands using in NMR assignments.

Table 1X-ray diffraction data of $[\text{Cu}^{\text{I}}(2,2'\text{-biquinoline})(1,2\text{-bis}(\text{diphenylphosphino})\text{ethane})](\text{ClO}_4)$.

Crystal description	prism
Cell setting	monoclinic
Space group	$P2_1/n$
Formula weight	817.69
Chemical formula	$\text{C}_{44}\text{H}_{36}\text{ClCuN}_2\text{O}_4\text{P}_2$
a (Å)	14.8285(5)
b (Å)	16.4564(6)
c (Å)	15.6263(5)
β (°)	92.486(4)
V (Å ³)	3809.6(4)
Z	4
Crystal size (mm)	$0.36 \times 0.27 \times 0.21$
δ (g/cm ³)	1.426
μ (mm ⁻¹)	0.774
T (K)	125
$F(0\ 0\ 0)$	1688
θ Range (°)	1.80–30.25
h, k, l	$0 > h > 20, 0 > k > 23, -21 > l > 21$
Reflections refined $I > 2\sigma(I)$	5996
Parameters	487
R_1, wR_2 (all data)	0.035, 0.062
Residuals (e Å ⁻³)	0.030, -0.120

Table 2Selected bond distances (Å) and angles (°) of $[\text{Cu}^{\text{I}}(2,2'\text{-biquinoline})(1,2\text{-bis}(\text{diphenylphosphino})\text{ethane})](\text{ClO}_4)$.

<i>Distances</i>	
Cu–N1	2.028(2)
Cu–N2	2.027(3)
Cu–P1	2.246(1)
Cu–P2	2.235(1)
C35–C36	1.473(5)
<i>Angles</i>	
N1–Cu–N2	81.0(1)
P1–Cu–P2	92.92(3)
N1–Cu–P1	119.09(6)
N1–Cu–P2	126.17(7)
N2–Cu–P1	112.22(7)
N2–Cu–P2	127.85(7)

Table 3Selected angles (°) and bond lengths (Å) of $[\text{Cu}^{\text{I}}(2,2'\text{-biquinoline})(\text{bis}(\text{diphenylphosphino})\text{alkane})](\text{ClO}_4)$ obtained with DFT or X-ray methods.

Alkyl method	Methyl DFT	Ethyl X-ray	Ethyl DFT	Butyl DFT
DHA	81.4	85.6	84.7	81.9
P–Cu–P	76.0	92.92(3)	91.7	109.3
N–Cu–N	81.0	81.0(1)	80.5	79.5
Cu–P1	2.337	2.246(1)	2.288	2.270
Cu–P2	2.333	2.235(1)	2.290	2.299
Cu–N1	2.060	2.028(2)	2.070	2.090
Cu–N2	2.060	2.027(3)	2.072	2.114
IQDH	5.6	10.4	6.9	12.8

2.2. Synthesis and characterization

$[\text{Cu}(\text{CH}_3\text{CN})_4]\text{ClO}_4$ was prepared according to the literature procedure [14]. All the solvents were dried and purified by standard methods. 2,2'-Biquinoline and alkyl-diphenylphosphines (Aldrich) reagents were used as received. The acetonitrile used for electrochemical studies was dried with CaH_2 and distilled prior to use.

2.3. General synthesis procedure for the $[\text{Cu}(\text{biq})(\text{bis}(\text{diphenylphosphine})\text{alkane})](\text{ClO}_4)$ complexes

About 0.050 g of $[\text{Cu}^{\text{I}}(\text{CH}_3\text{CN})_4](\text{ClO}_4)$ (0.15 mmol) dissolved in dichloromethane were added to a 100 mL three-neck reactor con-

taining 0.60 mmol of the corresponding bis(diphenylphosphine)alkane in dry dichloromethane under stirring and N_2 atmosphere at room temperature. After 1 h, 0.038 g of 2,2'-biquinoline (0.15 mmol) dissolved in 20 mL of dichloromethane were added dropwise. After the addition was completed (30 min approximately), the mixture was stirred for 4 h at room temperature. The orange solution was quickly filtered over powder cellulose and concentrated under reduced pressure to approximately 2 mL, then cooled to 4 °C followed by addition of cold diethyl ether to give the $[\text{Cu}^{\text{I}}(\text{biq})(\text{bis}(\text{diphosphine})\text{alkane})](\text{ClO}_4)$ complexes as a microcrystalline precipitate. Ether in excess was removed under reduced pressure.

2.3.1. $[\text{Cu}^{\text{I}}(\text{biq})(\text{bppm})](\text{ClO}_4)$

Yellow crystals, yield: 60%. Molar conductivity (acetone): $103.0 \text{ S cm}^2 \text{ mol}^{-1}$. M.p. 127 °C (dec.). *Anal.* Calc. for $(\text{CuC}_{43}\text{H}_{34}\text{N}_2\text{O}_4\text{P}_2\text{Cl})$: C, 64.26; N, 3.49; H, 4.26. Found: C, 64.47; N, 3.42; H, 4.67%. Mass spectra: $m/z = 703.1$. ^{31}P NMR (CDCl_3): -16.71 ppm.

2.3.2. $[\text{Cu}^{\text{I}}(\text{biq})(\text{bppe})](\text{ClO}_4)$

Red crystals, yield: 75%. Molar conductivity (acetone): $102.2 \text{ S cm}^2 \text{ mol}^{-1}$. M.p. 183 °C (dec.). *Anal.* Calc. for $(\text{CuC}_{44}\text{H}_{36}\text{N}_2\text{O}_4\text{P}_2\text{Cl})$: C, 64.63; N, 3.43; H, 4.44. Found: C, 64.98; N, 3.37; H, 4.77%. Mass spectra: $m/z = 717.2$. ^{31}P NMR (CDCl_3): -10.10 ppm.

2.3.3. $[\text{Cu}^{\text{I}}(\text{biq})(\text{bppb})](\text{ClO}_4)$

Orange crystals, yield: 80%. Molar conductivity (acetone): $105.7 \text{ S cm}^2 \text{ mol}^{-1}$. M.p. 144 °C (dec.). *Anal.* Calc. for $(\text{CuC}_{46}\text{H}_{40}\text{N}_2\text{O}_4\text{P}_2\text{Cl})$: C, 65.32; N, 3.31; H, 4.77. Found: C, 65.25; N, 3.31; H, 4.88%. Mass spectra: $m/z = 745.2$. ^{31}P NMR (CDCl_3): -12.50 ppm.

3. Results and discussion

The reaction of one equivalent of $[\text{Cu}(\text{CH}_3\text{CN})_4](\text{ClO}_4)$ with two equivalents of the respective bis(diphenylphosphino)alkane ligand (Fig. 1), afforded the $[\text{Cu}^{\text{I}}(\text{bis}(\text{diphenylphosphine})\text{alkane})_2](\text{ClO}_4)$ complexes in colorless solutions. The addition of one equivalent of 2,2'-biquinoline dissolved in dichloromethane yielded colored solutions, from which the complexes were obtained as microcrystalline powder by precipitation with cold diethyl ether.

Conductivity measurements show a 1:1 ionic ratio for all the complexes, which is in agreement with mass results (see above) for mononuclear species. The complexes are air stable both in solid and in solution phase in most of the commonly used solvents, do not experiencing chemical changes in solution during the time required for each experiment, as it has been reported for related systems [5,15].

3.1. Description of the crystal structure

The crystal structure shows a discrete mononuclear $[\text{Cu}(\text{biq})(\text{bppe})]^+$ cation complex, with the perchlorate ion located between the aromatic rings of 2,2'-biquinoline and 1,2-bis-diphosphine ligands. The cation coordination geometry corresponds to a distorted CuN_2P_2 tetrahedron. A side view of the molecule showing anisotropic ellipsoids and labelling is depicted in Fig. 2.

Selected bond angles and bond distances are given in Table 2. The average Cu–N and Cu–P distances are 2.028(2) and 2.240(1) Å, respectively, and are within the observed range for similar heteroleptic copper(I) species containing substituted phenanthrolines instead of biquinolines [9,16], whose variation is in the Cu–N range from 2.02 to 2.07 Å [17], while in $[\text{Cu}(\text{L})_2]^+$ complexes, $\text{L} = 3,3'$ -substituted-2,2'-biquinoline, the Cu–N bond

lengths vary according to the ligand substituent. The Cu–P distances in $[\text{Cu}(\text{biq})(\text{bppe})]^+$ are slightly different to each other (Cu–P1 = 2.235(1) and Cu–P2 = 2.246(1) Å), but they fall in the range of reported data for related bis-diphosphine copper complexes. For example, in the closely related cationic complex (1,3-bis(diphenylphosphino)propane)-(2,9-dimethyl-1,10-phenanthroline)-copper(I) hexafluorophosphate, they are 2.261(1) and 2.227(1) Å, confirming the difference between Cu–P bond lengths. Interestingly, in the less symmetric complex $[\text{Cu}(\text{pymtH})(\text{dppp})\text{Cl}]$ (pymtH = pyrimidine-2-thione, dppp = bis(diphenylphosphino)propane) both Cu–P bond lengths are equal, 2.276(1) Å [18], and so a more symmetric complex displays different Cu–P bonds whereas for a more asymmetric complex there is Cu–P bond length equivalence.

The bite angle N1–Cu–N2, 81.0(1)°, is comparable to that observed in the heteroleptic complex $[\text{Cu}(\text{dmp})(\text{PPh}_3)_2]^+$, 80.5° (9) (dmp = 2,9-dimethyl-1,10-phenanthroline). The dihedral angle (DHA) of the complex, defined between the planes N1–Cu–N2 and P1–Cu–P2, is 85.6°, indicating deviation from the ideal tetrahedral value of 90°, expected for a copper(I) geometry. The interquinoline dihedral angle between planes of both quinoline moieties (IQDHA) is 10.4°. Table 3 indicates distortion from planarity for this ligand.

In addition, the torsion angle N1–C35–C36–N2 is 6.1°. This value is lower than those in the literature observed for several complexes; for example 8.3° in $\text{RuCl}_2(\text{NBD})(\text{biq})$ (NBD = Norbornadiene), 17.7° in $[\text{Re}(\text{CO})_3(\text{biq})(\text{py})](\text{CF}_3\text{SO}_3)$ (py = pyridine) and 12.1° and 17.4° for both isomers of $[\text{Re}(\text{CO})_3(\text{biq})(\text{Bzpy})](\text{CF}_3\text{SO}_3)$ (Bzpy = benzylpyridine) [19].

On the other hand, tension on the ethyl bridge can be observed through the angles P1–C25–C26 = 112.2° and C25–C26–P2 = 113.0°, as they are wider than the tetrahedral value. This seems to be confirmed by the torsion angle P1–C25–C26–P2 = 46.0° when compared with those of the two dppp complexes mentioned earlier that have two torsion angles larger than 70° and so the ethyl complex seems to have a more flattened alkyl link than the *n*-propyl ligand.

3.2. DFT calculations

The DFT optimized geometry of the $[\text{Cu}(\text{biq})(\text{bppe})]^+$ complex shows differences with its X-ray crystal structure, such as wider dihedral angle (DHA) and shorter Cu–P and Cu–N bond lengths than in the crystal structure, see Table 3. These may be due to a constrained structure in the crystal because of packing. An additional source of difference may be the electrostatic influence from the perchlorate environment, which is missing in the isolated cationic species from DFT calculation.

In the X-ray structure it is also noticeable a greater planarity distortion in the quinoline moieties of the $[\text{Cu}^{(I)}(\text{biq})(\text{bppe})](\text{ClO}_4)$ complex, (IQDHA of 10.4°) also observed in other complexes [19,20]. This is also probably due to crystal packing that is missing in the isolated DFT structure (IQDHA of 6.1°).

Despite the differences between DFT and X-ray structures of $[\text{Cu}^{(I)}(\text{biq})(\text{bppe})]^+$, useful information can be deduced when the optimized geometries of the three complexes are compared. First, no correlation is observed between the calculated dihedral angles, DHA, with the length of the inter-phosphorus chain (Table 3), having the **bppm** and **bppb** complexes similar DHA values.

In addition, the tension on the aliphatic inter-phosphorus bridge can be understood in terms of the angles in hetero-cycles formed by Cu–P₂–C_n atoms as shown in Fig. 3. For example, deviation from the ideal 109.5° value for the carbon atom are in the order: **bppm** (P–C–P = 100.53°) > **bppb** (P–(C)₄–P = 114–118°) > **bppe** (P–(C)₂–P = 112.64°) (Fig. 3). The tension on the aliphatic bridge could be responsible of the rearrangement process imposed on the complexes by the phosphine ligand, where the **bppm** complex should be the more restricted. This trend is also observed in solution phase, both spectroscopically (NMR and UV–Vis) and by cyclic voltammetry (see below).

3.3. NMR spectroscopy

Proton signal assignments were carried out by the concerted use of 1D and 2D NMR experiments that included 2D-COSY and

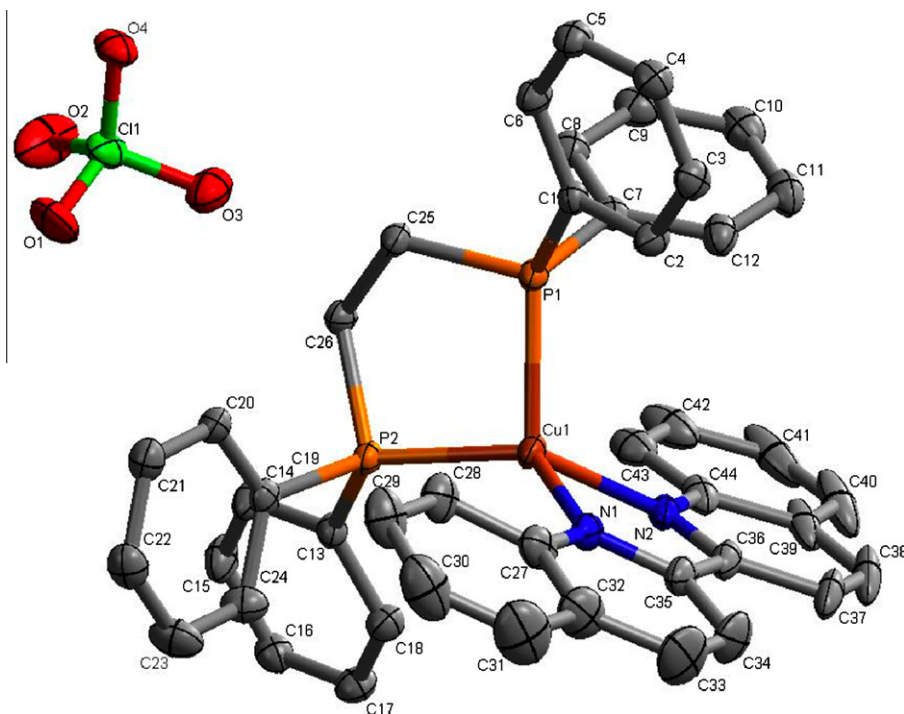


Fig. 2. X-ray crystal structure of the complex for $[\text{Cu}^{(I)}(2,2'\text{-biquinoline})(1,2\text{-bis(diphenylphosphino)ethane})](\text{ClO}_4)$ showing anisotropic ellipsoids and H atoms omitted for clarity.

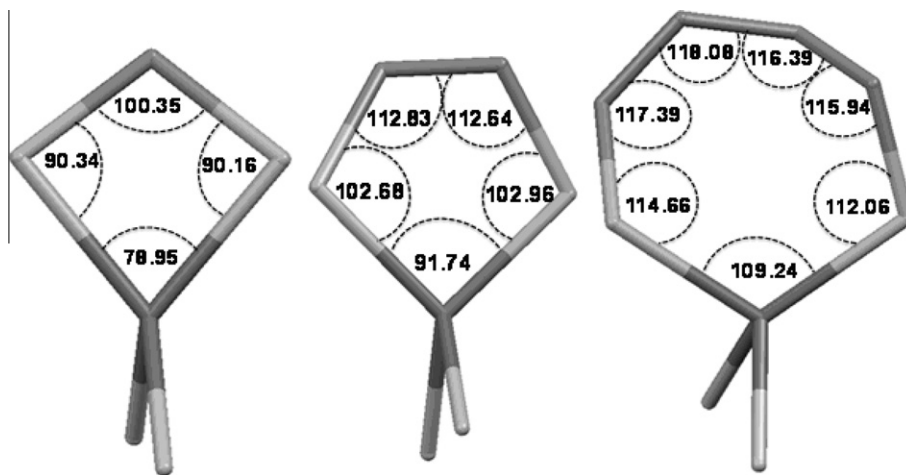


Fig. 3. DFT results for phosphine ligands, including P-Cu-P, in $[\text{Cu}^{\text{I}}(2,2'\text{-biquinoline})(\text{bis}(\text{diphenylphosphino})\text{alkane})](\text{ClO}_4)$ complexes.

2D-NOESY spectra. The chemical shift (δ in ppm) and $\Delta\delta$ ($\delta_{\text{complex}} - \delta_{\text{biq}}$) data for ^1H , of the free ligands and their corresponding complexes are summarized in Table 4.

^1H NMR signals pattern for biquinoline ligands are well known [19–22], corresponding to six aromatic resonances distributed in two doublets for AX spin system formed by H_3 and H_4 protons, and in a spin system formed by the remaining protons which are observed as two doublets for H_5 and H_8 , and two double-doublet (observed as a pseudo triplet) for H_6 , H_7 , protons (Table 4). However, the chemical shift for each proton in 2,2'-biquinoline is very sensitive to the distribution of the rest of the ligands in a complex. For this reason it was required 2D NMR experiments to obtain an unambiguous signal assignment.

Protons assignment of the coordinated biquinoline was performed as follows: H_4 and H_5 were identified through dipolar coupling provided by 2D-NOESY spectra. The AX system formed by H_3 and H_4 was then verified by scalar correlation in 2D-COSY spectra, which also provides the connectivity for assignments of H_5 – H_6 – H_7 – H_8 protons.

The protons in the inter-phosphorus chain of the bis-biphosphine-alkane ligands appear at higher field, with a correct relative integration for a mononuclear heteroleptic stoichiometry. However, these signals are broad and without fine structure (Fig. 4).

Similarly, the only signal observed in $^{31}\text{P}\{^1\text{H}\}$ NMR spectra of bis-biphosphine-alkane ligands in the complexes, is also a broad line that suggest a slow conformational motion of the alkane chain on the NMR timescale. The ^{31}P frequency in the complexes is con-

siderably shifted to lower field, c.a. 3.00 ppm compared to the free ligands, in agreement with the chemical shift observed in other Cu(I) complexes containing phosphine ligands. For example, the -10.10 ppm chemical shift observed for $[\text{Cu}^{\text{I}}(\text{biq})(\text{bpppe})]^+$ is comparable to the -10.56 ppm chemical shift previously reported for a related Cu(I) azine complex with the same bpppe ligand [9].

The aromatic proton signals of the phosphine ligands are poorly differentiated compared to those in biquinoline ligand. However, it is possible to observe NOESY correlations between H_α and H_β in two of the three complexes which can be used for structural assignment in the complex.

Contrary to the deshielding effect over the 2,2'-biquinoline protons expected by the metal complexation, some protons are high field shifted (see $\Delta\delta$ in Table 4). H_7 and H_8 are the most shielded protons because they are the closest ones to the copper atom. The high sensitivity of these protons respect to the structure in biquinoline complexes has been well established in a previous work [19–22].

This behavior could be explained by the spatial arrangement of both ligands in the complexes, where H_7 and H_8 protons would lie in the shielded region of some aromatic rings of bis-biphosphines-alkane ligand.

Based on the X-ray crystal structure of $[\text{Cu}^{\text{I}}(\text{biq})(\text{bpppe})]^+$ and DFT calculations, the biquinoline ligand has only a slight deviation from coplanarity of their quinoline halves.

The X-ray structure suggests that the biphosphine is the ligand experiencing most of the conformational rearrangement in

Table 4

^1H NMR chemical shifts for ligands and complexes.

Compound	Chemical shifts/ppm (multiplicity)										
	Aromatic protons									Aliphatic inter-phosphorus bridge	
	H_3	H_4	H_5	H_6	H_7	H_8	H_α	H_β	H_γ	H_a	H_b
2,2'-Biquinoline	8.85 (d)	8.30 (d)	7.86 (d)	7.58 (t)	7.75 (t)	8.25 (d)					
$[\text{Cu}(\text{biq})(\text{bppm})](\text{ClO}_4)$	8.85 (d)	8.33 (d)	8.23 (d)	7.76 (t)	7.58 (t)	7.89 (d)	7.09 (m)	6.95 (t)	7.09 (m)	3.21 (s)	
(bppm)							7.43 (m)	7.29 (m)	7.29 (m)	2.81 (s)	
$\Delta\delta^a$	0	0.03	0.37	0.18	-0.17	-0.36					
$[\text{Cu}(\text{biq})(\text{bpppe})](\text{ClO}_4)$	8.97 (d)	8.79 (d)	7.98 (d)	7.49 (t)	6.96 (t)	7.43 (d)	7.20 (d)	7.07 (t)	7.31 (t)	2.47 (dd)	
(bpppe)							7.34 (m)	7.34 (m)	7.34 (m)	2.10 (t)	
$\Delta\delta$	0.12	0.49	0.12	-0.09	-0.79	-0.82					
$[\text{Cu}(\text{biq})(\text{bppb})](\text{ClO}_4)$	8.74 (d)	8.61 (d)	7.87 (d)	7.51 (t)	7.30 (t)	7.81 (d)	7.02 (d)	6.90 (t)	7.06 (t)	2.79 (t)	2.34 (t)
(bppb)							7.37 (m)	7.33 (m)	7.33 (m)	2.02 (t)	1.56 (m)
$\Delta\delta$	-0.11	0.31	0.01	-0.07	-0.45	-0.44					

δ are informed relative to $\text{Si}(\text{CH}_3)_4$ at 300 K in CDCl_3 .

^a $\Delta\delta = \delta_{\text{complex}} - \delta_{\text{biquinoline}}$.

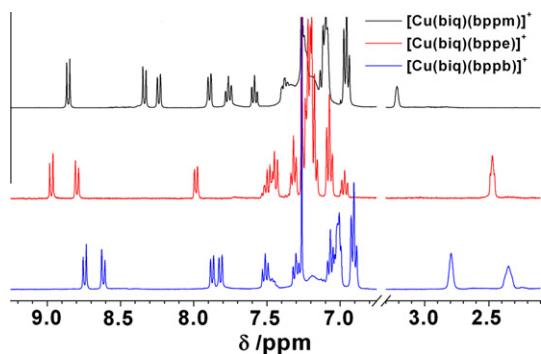


Fig. 4. ^1H NMR spectra for $[\text{Cu}^{\text{I}}(2,2'\text{-biquinoline})(\text{bis}(\text{diphenylphosphino})\text{alkane})](\text{ClO}_4)$ complexes recorded at 300 K in CDCl_3 .

$[\text{Cu}^{\text{I}}(\text{biq})(\text{bppe})]^+$ complex in response to the coordination geometry requirements of the copper. Furthermore, in the crystal structure Fig. 2, it can be observed that H_7 and H_8 are between two phenyl rings of the **bppe** ligand, where the magnetic currents shield both protons.

The $\Delta\delta$ values of H_7 and H_8 protons along the series of complexes (see Table 4), show no direct correlation with the inter-phosphorus chain length. In effect, the shielding for these protons increases in the following order $[\text{Cu}^{\text{I}}(\text{biq})(\text{bppm})](\text{ClO}_4) < [\text{Cu}^{\text{I}}(\text{biq})(\text{bppb})](\text{ClO}_4) < [\text{Cu}^{\text{I}}(\text{biq})(\text{bppe})](\text{ClO}_4)$.

The chemical shifts of the H_7 and H_8 protons are in direct relation with their orientation toward shielding currents of phenyl ring, which can be determined by effect of the alkyl bridge length over the complex geometry. Consequently, the decreasing in the frequency difference ($\Delta\delta$ between H_7 and H_8 protons can be indicative of a tetrahedral geometry distortion, which favor the collapse of phenyl ring toward quinoline fragments in the order observed (see above) for this series of complexes.

3.4. UV–Vis spectroscopy

Electronic spectra data of the complexes and ligands in acetone, tetrahydrofuran, and chloroform are shown in Table 5.

The spectral region below 400 nm is dominated by intense $\pi \rightarrow \pi^*$ intraligand transition bands, which are similar to the spectrum of the free biquinoline ligand [19–22]. These bands undergo a red-shift upon complexation to copper(I). A lower energy metal to ligand charge transfer band (MLCT) is observed in the range 400–500 nm for the complexes (Fig. 4), corresponding to a transition from the HOMO orbital centered in Cu atom (d^{10} full shell), toward a π^* -biquinoline orbital [23]. This assignment is supported by the sensitivity observed for this band to the polarity of the solvents and by their position in the spectra, in agreement with the fact that the LUMO is a π^* antibonding orbital of the

2,2'-biquinoline, due to their higher π delocalization in comparison with the phenyl groups of the biphosphine ligands [23]. In addition, the Cu(I) to bis-biphosphine-alkane charge transfer are expected to appear overlapped by the more intense intraligand biquinoline absorption bands (about 350 nm).

The MLCT band of the heteroleptic complexes are shifted 50–100 nm toward short wavelengths compared to the homoleptic $[\text{Cu}(\text{biq})_2]^+$ complex (λ_{max} TCML is 550 nm), in accordance to the greater π -acceptor nature of phosphorus in the biphosphine ligand respect to biquinoline [23a].

Furthermore Fig. 5 and Table 5, show a notorious shifting of metal to ligand charge transfer band (MLCT) at longer wavelength in the order $[\text{Cu}^{\text{I}}(\text{biq})(\text{bppm})](\text{ClO}_4) < [\text{Cu}^{\text{I}}(\text{biq})(\text{bppb})](\text{ClO}_4) < [\text{Cu}^{\text{I}}(\text{biq})(\text{bppe})](\text{ClO}_4)$.

Considering the MLCT as a process occurring between copper and the biquinoline ligand, it can be seen that distortions imposed by the bis-biphosphine-alkane ligand modify the energy level distribution in the complexes. Then, the red-shifting of MLCT must be due to the HOMO destabilization which reduces the necessary energy to reach the excited states.

In addition, the tension imposed by the aliphatic bridge in the diphosphine could restrict the conformational changes. Consequently, it has not been observed a linear correlation between lengths of the alkane chain and both the MLCT energy and ^1H NMR results (see above).

3.5. Cyclic voltammetry

Electrochemical properties were determined by cyclic voltammetry in acetonitrile solution, under nitrogen at room temperature

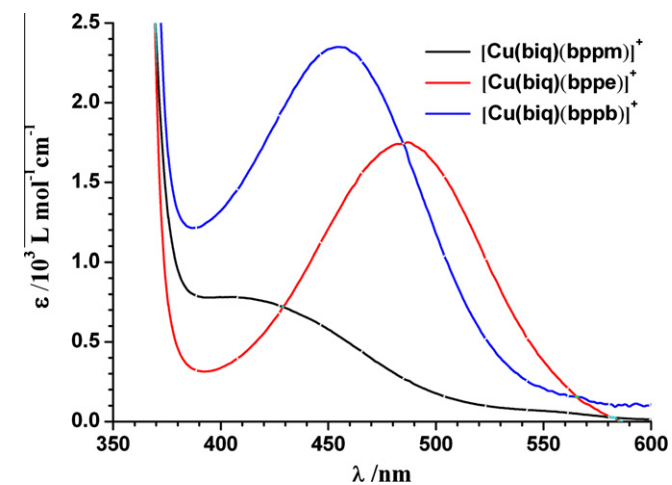


Fig. 5. UV–Vis spectra of the complexes in acetone, in the region of the metal to ligand charge transfer band.

Table 5
UV–Vis data for the $[\text{Cu}^{\text{I}}(\text{biq})\text{L}](\text{ClO}_4)$ complexes in solution.

Ligand (L)	Solvent	$\lambda_{\text{abs}}/\text{nm}$ ($10^{-2} \epsilon/\text{L mol}^{-1} \text{cm}^{-1}$)	
		$\text{Cu}^{\text{I}} \rightarrow \text{biq}$	$(\pi \rightarrow \pi^*)$
bppm	$(\text{CH}_3)_2\text{CO}$	411 (7.82)	360 (82.06), 344 (66.51), 330 (sh)
	THF	431 (sh)	360 (53.29), 340 (68.13), 326 (71.74)
	CHCl_3	430 (sh)	361 (87.93), 346 (73.14)
bppe	$(\text{CH}_3)_2\text{CO}$	486 (17.53)	361 (104.62), 343 (99.76), 332 (sh)
	THF	484 (19.64)	362 (117.99), 345 (11.037), 332 (sh)
	CHCl_3	476 (23.68)	362 (136.72), 346 (12.209), 333 (sh)
bppb	$(\text{CH}_3)_2\text{CO}$	450 (23.49)	360 (147.98), 344 (12.678)
	THF	456 (19.54)	361 (136.27), 345 (11.451)
	CHCl_3	451 (21.54)	361 (149.74), 346 (12.589)

sh: Shoulder.

Table 6Cyclic voltammetry results of $[\text{Cu}^{\text{I}}(2,2'\text{-biquinoline})(\text{bis}(\text{diphenylphosphino})\text{alkane})](\text{ClO}_4)$ complexes^a.

Complexes	$E_{1/2}^{\text{b}}$ (V)		Oxidation ^d
	Reduction ^c		
$[\text{Cu}^{\text{I}}(\text{biq})(\text{bppm})](\text{ClO}_4)$	-1.57	-1.16	1.23
$[\text{Cu}^{\text{I}}(\text{biq})(\text{bppe})](\text{ClO}_4)$	-1.64	-1.15	1.10
$[\text{Cu}^{\text{I}}(\text{biq})(\text{bppb})](\text{ClO}_4)$	-1.55	-1.19	1.14

^a In acetonitrile at room temperature.^b Potential measurements are referred to the Ag/AgCl, in 10^{-1} mol/L tetraethylammoniumperchlorate/acetonitrile solution at room temperature.^c $E_{1/2} = \frac{1}{2}(E_{\text{pc}} - E_{\text{pa}})$ to scan rate of 20 mV s^{-1} .^d $E_{1/2} = \frac{1}{2}(E_{\text{pc}} - E_{\text{pa}})$ to scan rate of 100 mV s^{-1} .

in -2.00 to $+2.00$ V versus SCE potential range (Table 6). Fig. 6 shows a representative cyclic voltammogram for $[\text{Cu}^{\text{I}}(\text{biq})(\text{bppb})](\text{ClO}_4)$.

The complexes show a single anodic peak for the Cu(I) oxidation process around 1.20 V, the scan rate being 20 mV s^{-1} [7,24]. Scanning anodically from 0.00 to 2.00 V, only a cathodic peak is observed for the Cu(II)/Cu(I) redox process. Scan rate dependence suggest that the copper complexes are oxidized in an irreversible diffusion-controlled step process [25]. These oxidation potentials compare well to those reported for similar systems [24,25].

The potentials values observed for this process shows the following trend: $[\text{Cu}^{\text{I}}(\text{biq})(\text{bppe})](\text{ClO}_4)$, +1.10 V; $[\text{Cu}^{\text{I}}(\text{biq})(\text{bppb})](\text{ClO}_4)$, +1.14 V; $[\text{Cu}^{\text{I}}(\text{biq})(\text{bppm})](\text{ClO}_4)$, +1.23 V. The trend in the positive potential values is coincident with the spectroscopic result previously discussed (UV-Vis and NMR).

Furthermore, shifting to more positive potential has been usually associated to an essentially tetrahedral surrounding around the metal center [7,8].

The complexes show two successive reduction processes in the 0.0 – -2.0 V range, which are centered in $E_{1/2} = -1.17$ V and $E_{1/2} = -1.60$ V potential values. The first reduction couple shows ΔE_{p} values concordant with a quasi-reversible process, which corresponds to the addition of one electron to a π^* orbital of the coordinated biquinoline ligand (biq/biq^-) in agreement with the potential values reported for several biquinoline complexes. Also, this fact is in agreement with the highest π delocalization of biquinoline respect to phosphine ligands, supporting experimentally that LUMO is the π^* orbital of the biquinoline ligand. Further support for this assignment comes from the good linear correlation

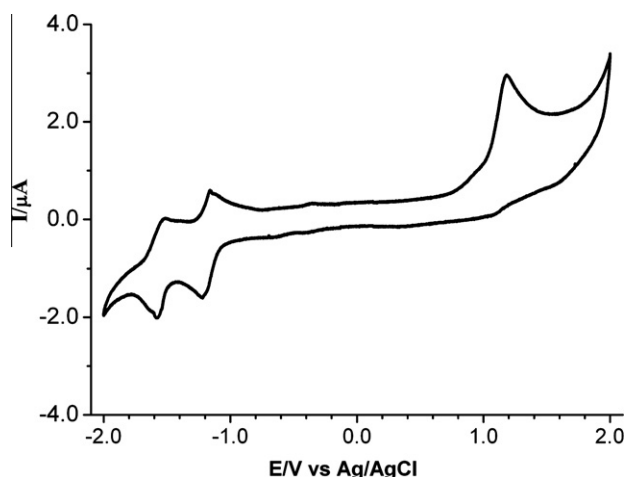


Fig. 6. Cyclic voltammogram for $[\text{Cu}^{\text{I}}(2,2'\text{-biquinoline})(1,4\text{-bis}(\text{diphenylphosphine})\text{butane})](\text{ClO}_4)$ in acetonitrile. Speed sweep, 20 mV s^{-1} .

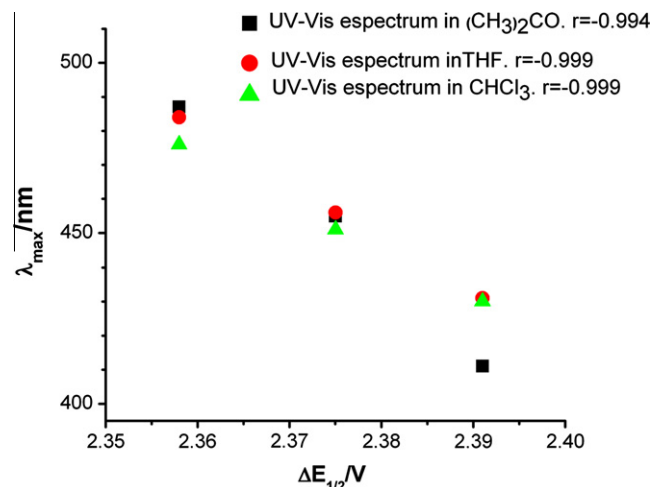


Fig. 7. $\Delta E_{1/2}$ vs. absorption maxima to MLCT.

observed between the energy of the MLCT band and $\Delta E_{1/2}$, where $\Delta E_{1/2} = E_{1/2}(\text{oxidation}) - E_{1/2}(\text{first reduction})$ (Fig. 7).

It is expected that the first reduction potential be dependent on the coplanarity of the quinoline moieties, since greater interquinoline dihedral angle (more distortion) drives to the loss of electronic conjugation on the ligand and consequently more negative potential values [22,23]. Thus, the biq/biq^- couple is indicative of the coplanarity degree of both quinolines halves. Therefore, the small differences in the reduction potentials through the series is another evidence that biquinoline is not the ligand that experience the most important structural changes, while the conformational rearrangement of the diphosphine ligands seems to be the main responsible of variations in the HOMO energy along the complexes series.

Optimized geometries support the fact that the **bppm** and **bppe** complexes have similar IQDHA (5.6° and 6.9° respectively) and also similar first reduction potential values (-1.16 and -1.15 V respectively), while the wider calculated IQDHA of the **bppb** complex (12.8°) could justify the more negative potential value.

The more negative reduction process could be tentatively assigned to the addition of a second electron to biquinoline ($\text{biq}^-/\text{biq}^{2-}$), over other possible processes, such as phosphine ligand or metal-centered Cu(I)/Cu(0) reductions. The difference about 500 mV between the first and the second wave has been used to support this assignment [19,20,22,23,26]. On the other hand, the voltammograms do not show characteristic peaks which could be assigned to a demetalation, Cu(I) to Cu(0), process.

4. Conclusions

The experimental results obtained by cyclic voltammetry and UV-Vis, processes involving charge transfer, either electrochemically or by light absorption, could be tentatively associated to the ability of the phosphine to determine the global geometry of complexes. This influence is corroborated by NMR results which confirmed the importance of these structural considerations.

The geometry of the complexes arises from two combined effects, the requirements imposed by the cation for a tetrahedral coordination and the tension produced by length of the alkane chain.

In summary, the experimental results are product of inter-phosphorus chain that induce several effects, that include bond distances, bond angles, modification in π backbonding among others, that influences the HOMO and LUMO orbitals, which are

not possible to be evaluated by considering only the micro environment of copper.

Acknowledgments

We are grateful for the provided support by DICYT USACH, FONDECYT No. 1101029 and MECESUP-0007 for NMR spectrometer. US National Science Foundation through Grant 0521237, for X-ray diffractometer.

Appendix A. Supplementary material

CCDC 775226 contains the supplementary crystallographic data for this paper. These data can be obtained free of charge from The Cambridge Crystallographic Data Centre via www.ccdc.cam.ac.uk/data_request/cif. Supplementary data associated with this article can be found, in the online version, at [doi:10.1016/j.ica.2010.07.032](https://doi.org/10.1016/j.ica.2010.07.032).

References

- [1] (a) S. Haneda, Y. Adachi, M. Hayashi, *Tetrahedron* 65 (2009) 10459; (b) Y. Liang, H. Zhou, Z.X. Yu, *J. Am. Chem. Soc.* 131 (2009) 17783; (c) B. Jiang, H. Tian, Z.G. Huang, M. Xu, *Org. Lett.* 10 (2008) 2737.
- [2] (a) C. Marzano, M. Pellei, S. Alidori, A. Brossa, G. Lobbia, F. Tisato, C. Santini, *Inorg. Biochem.* 100 (2006) 299; (b) M. Pellei, G. Lobbia, C. Santini, R. Spagna, M. Camalli, D. Fedeli, G. Falcioni, *Dalton Trans.* (2004) 2822; (c) M. McKeage, P. Papathanasiou, G. Salem, A. Sjaarda, G. Swiegers, P. Waring, S. Wild, *Met. Based Drugs* 5 (1998) 217.
- [3] (a) L. Qin, Q. Zhang, W. Sun, J. Wang, C. Lu, Y. Cheng, L. Wang, *Dalton Trans.* (2009) 9388; (b) S. Harkins, J. Peters, *J. Am. Chem. Soc.* 127 (2005) 2030; (c) H. Araki, K. Tsuge, Y. Sasaki, S. Ishizaka, N. Kitamura, *Inorg. Chem.* 44 (2005) 9667; (d) D. Cuttall, S. Kuang, P. Fanwick, D. McMillin, R. Walton, *J. Am. Chem. Soc.* 124 (2002) 6; (e) H. Song, Q. Wang, Z. Zhang, T. Mak, *Chem. Commun.* (2001) 1658; (f) D. Scaltrito, D. Thompson, J. O'Callaghan, G. Meyer, *Coord. Chem. Rev.* 208 (2000) 243.
- [4] (a) L. Lemus, J. Guerrero, J. Costamagna, G. Estiu, G. Ferraudi, A.G. Lappin, A. Oliver, B.C. Noll, *Inorg. Chem.* 49 (2010) 4023; (b) J.P. Collin, F. Durolo, J. Lux, J.P. Sauvage, *New J. Chem.* 34 (2010) 34; (c) C. Piguet, M. Borkovec, J. Hamacek, K. Zeckert, *Coord. Chem. Rev.* 249 (2005) 705; (d) M. Elhabiri, A.M. Albrecht-Gary, *Coord. Chem. Rev.* 252 (2008) 079.
- [5] (a) C. Palmer, D. McMillin, *Inorg. Chem.* 26 (1987) 3837; (b) S.M. Kuang, D.G. Cuttall, D.R. McMillin, P.E. Fanwick, R.A. Walton, *Inorg. Chem.* 41 (2002) 3313.
- [6] (a) M. Miller, P. Gantzel, T. Karpinsin, *Inorg. Chem.* 37 (1998) 2285; (b) D. McMillin, K. McNett, *Chem. Rev.* 98 (1998) 1201. and references therein.
- [7] E.C. Riesgo, Y.Z. Hu, F. Bouvier, R.P. Thummel, D.V. Scaltrito, G.J. Meyer, *Inorg. Chem.* 40 (2001) 3413.
- [8] (a) M. Miller, P. Gantzel, T. Karpinsin, *Inorg. Chem.* 38 (1999) 3414; (b) M. Eggleston, D. McMillin, K. Koeing, A. Pallenberg, *Inorg. Chem.* 36 (1997) 172.
- [9] T. McCormick, W.L. Jia, S. Wang, *Inorg. Chem.* 45 (2006) 147.
- [10] M. Camalli, R. Spagna, *J. Appl. Crystallogr.* 27 (1994) 861.
- [11] Materials Studio Visualizer, Accelrys Software Inc.: 10188 Telesis Court, Suite 100, San Diego, CA 92121, USA.
- [12] J.P. Perdew, J.A. Chevary, S.H. Vosko, K.A. Jackson, M.R. Pederson, D.J. Singh, C. Fiolhais, *Phys. Rev. B: Condens. Mater. Mater. Phys.* 46 (1992) 6671.
- [13] J.P. Perdew, K. Burke, M. Ernzerhof, *Phys. Rev. Lett.* 78 (1997) 1396E.
- [14] G. Kubas, *J. Inorg. Synth.* 19 (1979) 90.
- [15] R. Rader, D. McMillin, M. Buckner, T. Matthews, D. Casadonte, R. Lengel, S. Whittaker, L. Darmon, F. Lytle, *J. Am. Chem. Soc.* 103 (1981) 5906.
- [16] (a) Q. Zhang, J. Ding, Y. Cheng, L. Wang, Z. Xie, X. Jing, F. Wang, *Adv. Funct. Mater.* 17 (2007) 2983; (b) M. Navarro, O. Corona, T. González, *Acta Crystallogr., Sect. E63* (2007) 1153.
- [17] (a) P. Healy, L. Engelhardt, V. Patrick, A. White, *J. Chem. Soc., Dalton Trans.* (1985) 2541; (b) F. Klemens, P. Fanwick, J. Bibler, D. McMillin, *Inorg. Chem.* 28 (1989) 3076; (c) M. Geoffroy, M. Wermeille, C. Buchecker, J.P. Sauvage, G. Bernardinelli, *Inorg. Chim. Acta* 167 (1990) 157.
- [18] A. Paraskevas, J. Philip, P.J. Cox, S. Divanidis, A.C. Tsiapis, *Inorg. Chem.* 41 (2002) 6875.
- [19] (a) S. Moya, J. Guerrero, F. Rodriguez-Nieto, E. Wolcan, M. Félix, R. Baggio, M. Garland, *Helv. Chim. Acta* 88 (2005) 2842; (b) J. Guerrero, L. Fariás, L. Lemus, A. Quintanilla, A. Mena, L. Cortez, R. Baggio, M. Garland, *Polyhedron* 25 (2006) 9.
- [20] (a) J. Guerrero, S.A. Moya, R. Baggio, M. Garland, *Acta Crystallogr., Sect. C54* (1998) 1592; (b) J. Guerrero, S.A. Moya, M. Garland, R. Baggio, *Acta Crystallogr., Sect. C* 55 (1999) 932.
- [21] R.P. Thummel, F. Leufohn, *Inorg. Chem.* 26 (1987) 675.
- [22] S.A. Moya, J. Guerrero, R. Pastene, R. Sartori, R. Schmidt, R. Sariago, J. Sanz-Aparicio, I. Fonseca, M. Martinez-Ripoll, *Inorg. Chem.* 33 (1994) 2341.
- [23] (a) Y. Jahng, J. Hazelrigg, D. Kimball, E. Riesgo, F. Wu, R.P. Thummel, *Inorg. Chem.* 36 (1997) 5390; (b) W.F. Fu, X. Gan, J. Jiao, Y. Chen, M. Yuan, S.M. Chi, M.M. Yu, S.X. Xiong, *Inorg. Chim. Acta* 360 (2007) 2758.
- [24] S.M. Scott, K.C. Gordon, A.K. Burrell, *Inorg. Chem.* 35 (1996) 2452.
- [25] L. Douce, L. Charbonniere, M. Cesario, R. Ziessel, *New J. Chem.* 25 (2001) 1024.
- [26] (a) R. Lin, Y. Fu, C. Brock, T. Guarr, *Inorg. Chem.* 31 (1992) 4336; (b) M. DeArmond, K. Hanck, D. Wertz, *Coord. Chem. Rev.* 64 (1985) 65; (c) J. Cooper, D. MacQueen, J. Petersen, D. Wertz, *Inorg. Chem.* 29 (1990) 3701.